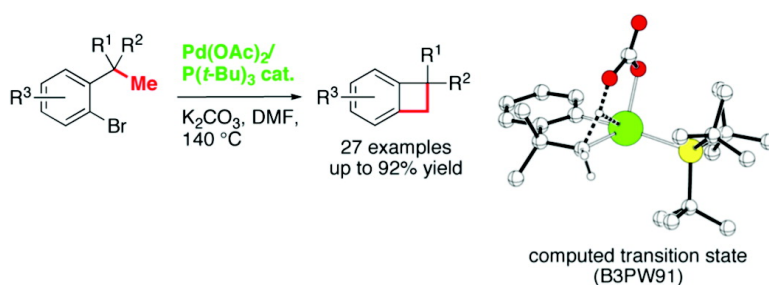


## Synthesis of Benzocyclobutenes by Palladium-Catalyzed C#H Activation of Methyl Groups: Method and Mechanistic Study

Manon Chaumontet, Riccardo Piccardi, Nicolas Audic, Julien Hitce, Jean-Louis Peglion, Eric Clot, and Olivier Baudoin

*J. Am. Chem. Soc.*, **2008**, 130 (45), 15157-15166 • DOI: 10.1021/ja805598s • Publication Date (Web): 18 October 2008

Downloaded from <http://pubs.acs.org> on February 8, 2009



### More About This Article

Additional resources and features associated with this article are available within the HTML version:

- Supporting Information
- Access to high resolution figures
- Links to articles and content related to this article
- Copyright permission to reproduce figures and/or text from this article

[View the Full Text HTML](#)

## Synthesis of Benzocyclobutenes by Palladium-Catalyzed C–H Activation of Methyl Groups: Method and Mechanistic Study

Manon Chaumontet,<sup>†</sup> Riccardo Piccardi,<sup>‡</sup> Nicolas Audic,<sup>†</sup> Julien Hitce,<sup>†</sup>  
Jean-Louis Peglion,<sup>§</sup> Eric Clot,<sup>\*,||</sup> and Olivier Baudoin<sup>\*,‡</sup>

*Institut Charles Gerhardt, UMR5253, CNRS-UM2-UMI-ENSCM, case courrier 1501, Place Eugène Bataillon, 34000 Montpellier, France, and Université Lyon 1, CNRS UMR5246, Institut de Chimie et Biochimie Moléculaires et Supramoléculaires, 43 Boulevard du 11 Novembre 1918, 69622 Villeurbanne, France*

Received July 18, 2008; E-mail: clot@univ-montp2.fr; olivier.baudoin@univ-lyon1.fr

**Abstract:** An efficient catalytic system has been developed for the synthesis of benzocyclobutenes by C–H activation of methyl groups. The optimal conditions employed a combination of Pd(OAc)<sub>2</sub> and P<sup>t</sup>Bu<sub>3</sub> as catalyst, K<sub>2</sub>CO<sub>3</sub> as the base, and DMF as solvent. A variety of substituted BCB were obtained under these conditions with yields in the 44–92% range, including molecules that are hardly accessible by other methods. The reaction was found limited to substrates bearing a quaternary benzylic carbon, but benzocyclobutenes bearing a tertiary benzylic carbon could be obtained indirectly from diesters by decarboxylation. Reaction substrates bearing a small substituent *para* to bromine gave an unexpected regioisomer that likely arose from a 1,4-palladium migration process. The formation of this “abnormal” regioisomer could be suppressed by introducing a larger substituent *para* to bromine. DFT(B3PW91) calculations on the reaction of 2-bromo-tert-butylbenzene with Pd(P<sup>t</sup>Bu<sub>3</sub>) with different bases (acetate, bicarbonate, carbonate) showed the critical influence of the coordination mode of the base to induce both an easy C–H activation and to allow for a pathway for 1,4-palladium migration. Carbonate is shown to be more efficient than the two other bases because it can abstract the proton easily and at the same time maintain  $\kappa^1$ -coordination without extensive electronic reorganization.

### Introduction

In recent years, transition-metal-catalyzed C–H activation has emerged as a powerful tool to transform otherwise unreactive C–H bonds into carbon–carbon or carbon–heteroatom bonds.<sup>1,2</sup> This new area of organic chemistry is gradually changing the way chemists functionalize molecules, providing atom- and step-economical alternatives to more traditional methods and facilitating the access to valuable and original compounds. In regard to the wealth of methods recently developed for the functionalization of arene and heteroarene C(sp<sup>2</sup>)-H bonds,<sup>3</sup> relatively little work has focused on the functionalization of unreactive alkyl C(sp<sup>3</sup>)-H bonds by catalytic C–H activation. Solutions to this rather difficult case have been proposed using either intramolecular activation, which can be

triggered by coordination of the metal to a directing group<sup>4,5</sup> or by oxidative addition,<sup>6,7</sup> or intermolecular, nondirected C–H activation.<sup>8</sup> We recently reported on the palladium-catalyzed C–H activation of benzylic alkyl groups borne by bromobenzenes **1** (eq 1).<sup>7</sup> In this case, the oxidative addition of the C–Br bond to palladium(0) triggers an intramolecular C–H activation to give a five or six-membered palladacyclic intermediate,

<sup>†</sup> Institut de Chimie des Substances Naturelles, CNRS UPR2301, avenue de la Terrasse, 91198 Gif-sur-Yvette, France.

<sup>‡</sup> Institut de Chimie et Biochimie Moléculaires et Supramoléculaires.

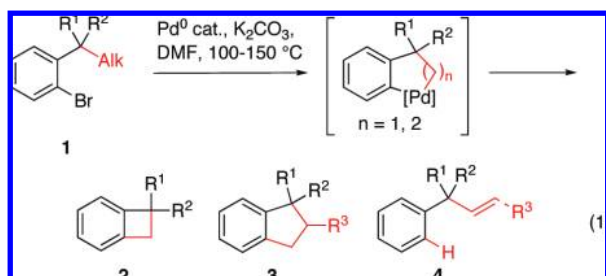
<sup>§</sup> Institut de Recherche Servier, 11 rue des Moulineaux, 92150 Suresnes, France.

<sup>||</sup> Institut Charles Gerhardt.

- (1) Selected reviews: (a) Dyker, G. *Angew. Chem., Int. Ed.* **1999**, *38*, 1698. (b) Kakiuchi, F.; Chatani, N. *Adv. Synth. Catal.* **2003**, *345*, 1077. (c) Dick, A. R.; Sanford, M. S. *Tetrahedron* **2006**, *62*, 2439. (d) Godula, K.; Sames, D. *Science* **2006**, *312*, 67.
- (2) In this article, C–H activation refers to transition-metal-catalyzed reactions that involve the cleavage of a C–H bond by an inner-sphere mechanism (see ref 1c). This definition excludes reactions that involve an outer-sphere mechanism, such as C–H insertions: (a) *Modern Rhodium-Catalyzed Organic Reactions*; Evans, P. A., Ed.; Wiley-VCH: Weinheim, 2005. (b) Davies, H. M. L.; Manning, J. R. *Nature* **2008**, *451*, 417. (c) Christmann, M. *Angew. Chem., Int. Ed.* **2008**, *47*, 2740.

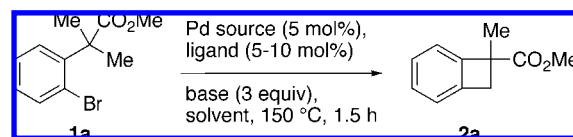
- (3) (a) Hassan, J.; Sévignon, M.; Gozzi, C.; Schulz, E.; Lemaire, M. *Chem. Rev.* **2002**, *102*, 1359. (b) Goj, L. A.; Gunnoe, T. B. *Curr. Org. Chem.* **2005**, *9*, 671. (c) Campeau, L.-C.; Fagnou, K. *Chem. Commun.* **2006**, 1253. (d) Alberico, D.; Scott, M. E.; Lautens, M. *Chem. Rev.* **2007**, *107*, 174. (e) Seregin, I. V.; Gevorgyan, V. *Chem. Soc. Rev.* **2007**, *36*, 1173.
- (4) (a) Chatani, N.; Asaumi, T.; Ikeda, T.; Yorimitsu, S.; Ishii, Y.; Kakiuchi, F.; Murai, S. *J. Am. Chem. Soc.* **2000**, *122*, 12882. (b) Zhang, X.; Fried, A.; Knapp, S.; Goldman, A. S. *Chem. Commun.* **2003**, 2060. (c) Murahashi, S.-I.; Komiya, N.; Terai, H.; Nakae, T. *J. Am. Chem. Soc.* **2003**, *125*, 15312. (d) DeBoef, B.; Pastine, S. J.; Sames, D. *J. Am. Chem. Soc.* **2004**, *126*, 6556. (e) Desai, L. V.; Hull, K. L.; Sanford, M. S. *J. Am. Chem. Soc.* **2004**, *126*, 9542. (f) Kakiuchi, F.; Tsuchiya, K.; Matsumoto, M.; Mizushima, E.; Chatani, N. *J. Am. Chem. Soc.* **2004**, *126*, 12792. (g) Giri, R.; Chen, X.; Yu, J.-Q. *Angew. Chem., Int. Ed.* **2005**, *44*, 2112. (h) Giri, R.; Liang, J.; Lei, J.-G.; Li, J.-J.; Wang, D.-H.; Chen, X.; Naggari, I. C.; Guo, C.; Foxman, B. M.; Yu, J.-Q. *Angew. Chem., Int. Ed.* **2005**, *44*, 7420. (i) Zaitsev, V. G.; Shabashov, D.; Daugulis, O. *J. Am. Chem. Soc.* **2005**, *127*, 13154. (j) Shabashov, D.; Daugulis, O. *Org. Lett.* **2005**, *7*, 3657. (k) Chen, X.; Goodhue, C. E.; Yu, J.-Q. *J. Am. Chem. Soc.* **2006**, *128*, 12634. (l) Giri, R.; Mangel, N.; Li, J.-J.; Wang, D.-H.; Breazzano, S. P.; Saunders, L. B.; Yu, J.-Q. *J. Am. Chem. Soc.* **2007**, *129*, 3510. (m) Campeau, L.-C.; Schipper, D. J.; Fagnou, K. *J. Am. Chem. Soc.* **2008**, *130*, 3266. (n) Mousseau, J. J.; Larivée, A.; Charette, A. B. *Org. Lett.* **2008**, *10*, 1641.

depending on the nature of the activated alkyl. This palladacycle subsequently evolves by intramolecular C–C coupling to give carbocycles **2–3** or  $\beta$ -H elimination to form olefins **4**. In particular, we were able to observe the direct formation of benzocyclobutenes **2** by C(sp<sup>3</sup>)-H activation of benzylic methyl groups.<sup>7a,6c,9</sup>



Benzocyclobutenes (BCB) are both important structural elements in active pharmaceutical ingredients and valuable intermediates for organic synthesis.<sup>10</sup> In particular, they undergo thermal electrocyclic ring-opening to give *ortho*-xylenes that can subsequently react in pericyclic reactions such as Diels–Alder cycloadditions.<sup>11</sup> This property was largely exploited in the past decades in the total synthesis of polycyclic natural products.<sup>10</sup> Despite their high synthetic value, very few general and chemoselective methods exist for the preparation of *functionalized* BCB, which seriously limits their availability and their use as synthetic intermediates. In this article, we describe a general method for the preparation of substituted BCB by

**Table 1.** Optimization of C–H Activation Reaction Parameters



entry	solvent	base	Pd source	ligand <sup>a</sup>	conversion (%) <sup>b</sup>	GC yield (%) <sup>b</sup>
1	DMF	K <sub>2</sub> CO <sub>3</sub>	Pd(OAc) <sub>2</sub>	P( <i>o</i> -tol) <sub>3</sub>	100	67
2	DMA	K <sub>2</sub> CO <sub>3</sub>	Pd(OAc) <sub>2</sub>	P( <i>o</i> -tol) <sub>3</sub>	72	38
3	NMP	K <sub>2</sub> CO <sub>3</sub>	Pd(OAc) <sub>2</sub>	P( <i>o</i> -tol) <sub>3</sub>	100	47
4	xylenes	K <sub>2</sub> CO <sub>3</sub>	Pd(OAc) <sub>2</sub>	P( <i>o</i> -tol) <sub>3</sub>	35	22
5	DMF	KHCO <sub>3</sub>	Pd(OAc) <sub>2</sub>	P( <i>o</i> -tol) <sub>3</sub>	80	51
6	DMF	Na <sub>2</sub> CO <sub>3</sub>	Pd(OAc) <sub>2</sub>	P( <i>o</i> -tol) <sub>3</sub>	40	9
7	DMF	Cs <sub>2</sub> CO <sub>3</sub>	Pd(OAc) <sub>2</sub>	P( <i>o</i> -tol) <sub>3</sub>	30	10
8	DMF	KF	Pd(OAc) <sub>2</sub>	P( <i>o</i> -tol) <sub>3</sub>	8	1
9	DMF	K <sub>3</sub> PO <sub>4</sub>	Pd(OAc) <sub>2</sub>	P( <i>o</i> -tol) <sub>3</sub>	54	14
10	DMF	KOAc	Pd(OAc) <sub>2</sub>	P( <i>o</i> -tol) <sub>3</sub>	7	1
11	DMF	<i>i</i> PrNEt <sub>2</sub>	Pd(OAc) <sub>2</sub>	P( <i>o</i> -tol) <sub>3</sub>	60	1
12	DMF	K <sub>2</sub> CO <sub>3</sub>	Pd <sub>2</sub> dba <sub>3</sub>	P( <i>o</i> -tol) <sub>3</sub>	100	70
13	DMF	K <sub>2</sub> CO <sub>3</sub>	PdCl <sub>2</sub> (MeCN) <sub>2</sub>	P( <i>o</i> -tol) <sub>3</sub>	100	73
14	DMF	K <sub>2</sub> CO <sub>3</sub>	PdCl <sub>2</sub> (MeCN) <sub>2</sub>	F-TOTP	88	52
15	DMF	K <sub>2</sub> CO <sub>3</sub>	PdCl <sub>2</sub> (MeCN) <sub>2</sub>	MeO-TOTP	100	71
16	DMF	K <sub>2</sub> CO <sub>3</sub>	PdCl <sub>2</sub> (MeCN) <sub>2</sub>	PPh <sub>3</sub>	23	2
17	DMF	K <sub>2</sub> CO <sub>3</sub>	PdCl <sub>2</sub> (MeCN) <sub>2</sub>	dppp <sup>d</sup>	19	1
18	DMF	K <sub>2</sub> CO <sub>3</sub>	PdCl <sub>2</sub> (MeCN) <sub>2</sub>	(C <sub>3</sub> PH)BF <sub>4</sub>	5	2
19	DMF	K <sub>2</sub> CO <sub>3</sub>	PdCl <sub>2</sub> (MeCN) <sub>2</sub>	DavePhos	43	13
20	DMF	K <sub>2</sub> CO <sub>3</sub>	PdCl <sub>2</sub> (MeCN) <sub>2</sub>	JohnPhos	100	89
21	DMF	K <sub>2</sub> CO <sub>3</sub>	PdCl <sub>2</sub> (MeCN) <sub>2</sub>	( <sup>t</sup> Bu <sub>3</sub> PH)BF <sub>4</sub>	100	93 (73) <sup>c</sup>
22	DMF	K <sub>2</sub> CO <sub>3</sub>	PdCl <sub>2</sub> (MeCN) <sub>2</sub>	Q-Phos	100	90
23	DMF	K <sub>2</sub> CO <sub>3</sub>	PdCl <sub>2</sub> (MeCN) <sub>2</sub>	IPr	26	8

<sup>a</sup> 10 or 5 mol% ligand for Pd<sup>II</sup> or Pd<sup>0</sup> source, respectively.

<sup>b</sup> Calculated using tetradecane as internal standard. Other observed products included the starting bromobenzene **1a** and the corresponding proto-debrominated product. <sup>c</sup> Yield of the isolated product. <sup>d</sup> 5 mol%.

- (5) Recent work in allylic C–H activation: (a) Chen, M. S.; Prabakaran, N.; Labenz, N. A.; White, M. C. *J. Am. Chem. Soc.* **2005**, *127*, 6970. (b) Delcamp, J. H.; White, M. C. *J. Am. Chem. Soc.* **2006**, *128*, 15076. (c) Olsson, V. J.; Szabó, K. *J. Angew. Chem., Int. Ed.* **2007**, *46*, 6891. (d) Fraunhoffer, K. J.; White, M. C. *J. Am. Chem. Soc.* **2007**, *129*, 7274. (e) Reed, S. A.; White, M. C. *J. Am. Chem. Soc.* **2008**, *130*, 3316. (f) Covell, D. J.; White, M. C. *Angew. Chem., Int. Ed.* **2008**, *47*, 6448.
- (6) (a) Dyker, G. *Angew. Chem., Int. Ed. Engl.* **1992**, *31*, 1023. (b) Dyker, G. *J. Org. Chem.* **1993**, *58*, 6426. (c) Dyker, G. *Angew. Chem., Int. Ed. Engl.* **1994**, *33*, 103. (d) Toivola, R. J.; Savilampi, S. K.; Koskinen, A. M. P. *Tetrahedron Lett.* **2000**, *41*, 6207. (e) Catellani, M.; Motti, E.; Ghelli, S. *Chem. Commun.* **2000**, 2003. (f) Solé, D.; Vallverdú, L.; Solans, X.; Font-Bardía, M. *Chem. Commun.* **2005**, 2738. (g) Barder, T. E.; Walker, S. D.; Martinelli, J. R.; Buchwald, S. L. *J. Am. Chem. Soc.* **2005**, *127*, 4685. (h) Dong, C.-G.; Hu, Q.-S. *Angew. Chem., Int. Ed.* **2006**, *45*, 2289. (i) Ren, H.; Knochel, P. *Angew. Chem., Int. Ed.* **2006**, *45*, 3462. (j) Ren, H.; Zi, L.; Knochel, P. *Chem. Asian J.* **2007**, *2*, 416. (k) Liron, F.; Knochel, P. *Tetrahedron Lett.* **2007**, *48*, 4943. (l) Lafrance, M.; Gorelsky, S. I.; Fagnou, K. *J. Am. Chem. Soc.* **2007**, *129*, 14570. (m) Dong, C.-G.; Hu, Q.-S. *Tetrahedron* **2008**, *64*, 2537. (n) Motti, E.; Catellani, M. *Adv. Synth. Catal.* **2008**, *350*, 565. (o) Watanabe, T.; Oishi, S.; Fujii, N.; Ohno, H. *Org. Lett.* **2008**, *10*, 1759. (p) Salcedo, A.; Neuville, L.; Zhu, J. *J. Org. Chem.* **2008**, *73*, 3600.
- (7) (a) Baudoin, O.; Herrbach, A.; Guéritte, F. *Angew. Chem., Int. Ed.* **2003**, *42*, 5736. (b) Hitce, J.; Retailleau, P.; Baudoin, O. *Chem.–Eur. J.* **2007**, *13*, 792. (c) Hitce, J.; Baudoin, O. *Adv. Synth. Catal.* **2007**, *349*, 2054.
- (8) (a) Baudry, D.; Ephritikhine, M.; Felkin, H.; Holmes-Smith, R. *J. Chem. Soc., Chem. Commun.* **1983**, 788. (b) Burk, M. J.; Crabtree, R. H. *J. Am. Chem. Soc.* **1987**, *109*, 8025. (c) Chen, H.; Schlecht, S.; Semple, T. C.; Hartwig, J. F. *Science* **2000**, *287*, 1995. (d) Lawrence, J. D.; Takahashi, M.; Bae, C.; Hartwig, J. F. *J. Am. Chem. Soc.* **2004**, *126*, 15334. (e) Murphy, J. M.; Lawrence, J. D.; Kawamura, K.; Incarvito, C.; Hartwig, J. F. *J. Am. Chem. Soc.* **2006**, *128*, 13684.
- (9) Catellani, M.; Ferioli, L. *Synthesis* **1996**, 769.
- (10) (a) Mehta, G.; Kotha, S. *Tetrahedron* **2001**, *57*, 625. (b) Sadana, A. K.; Saini, R. K.; Billups, W. E. *Chem. Rev.* **2003**, *103*, 1539.
- (11) (a) Oppolzer, W. A. *Synthesis* **1978**, 793. (b) Charlton, J. L.; Alauddin, M. M. *Tetrahedron* **1987**, *43*, 2873. (c) Nemoto, H.; Fukumoto, K. *Tetrahedron* **1998**, *54*, 5425.

palladium-catalyzed C–H activation. We show that this reaction is compatible with a number of functional groups, which should stimulate new developments in the chemistry of BCB. In addition, we report experimental observations and DFT calculations on the key C–H activation reaction that show for the first time the dual role of the carbonate base in the C–H bond cleavage as well as in palladium 1,4-migration.

## Results and Discussion

**1. Conditions Optimization.** We quickly discovered that the initial set of conditions that were used in our first report was not optimal for BCB synthesis (Table 1, entry 1).<sup>7a</sup> Using bromobenzene **1a** as model substrate for the C–H activation giving BCB **2a**, all reaction parameters were reinvestigated. Representative examples of modifications of the solvent, palladium source and ligand are listed in Table 1 with fixed temperature (150 °C) and reaction time (1.5 h). First, it appears that the nature of both the solvent (entries 1–4) and the base (entries 1, 5–11) is crucial to achieve high yields, DMF and potassium carbonate providing the optimal combination. It is noteworthy that the carbonate counteraction had also a major impact on the reaction efficiency (entries 1, 6–7). In contrast, the nature of the palladium source was relatively indifferent (entries 1, 12–13). Next, the palladium ligand was varied using dichlorobis(acetonitrile)palladium(II) as precatalyst (entries 13–23 and Figure 1). The nature of the ligand had again a profound influence on the reaction yield, with bulky, electron-rich monophosphines of the type RP<sup>t</sup>Bu<sub>2</sub> giving the highest yield in **2a** (entries 20–22). Among these,<sup>12</sup> tri-*tert*-butylphosphine,

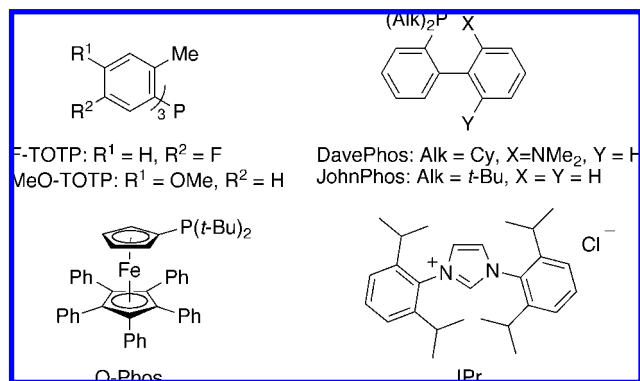
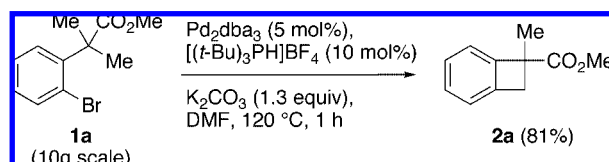


Figure 1. Ligands screened for C–H activation.

Scheme 1. Optimized Conditions for the Synthesis of BCB 2a



which was employed for convenience as its phosphonium salt,<sup>13</sup> proved the optimal ligand (entry 21). The higher activity of this ligand compared to the initial P(*o*-tol)<sub>3</sub> allowed us to decrease the reaction temperature down to 120 °C for the synthesis of **2a** (Scheme 1). The reaction, when performed on a 10 g scale (39 mmol of **1a**) using Pd<sub>2</sub>dba<sub>3</sub> (5 mol%)/(*t*-Bu<sub>3</sub>PH)BF<sub>4</sub> (10 mol%) as catalyst precursors and as low as 1.3 equiv potassium carbonate, gave BCB **2a** in a reproducible 81% yield.<sup>14</sup> This is the minimal temperature required for an efficient conversion of the substrate to the desired BCB product with this catalyst.

**2. Reaction Scope.** The formation of other substituted BCB by C(sp<sup>3</sup>)-H activation was next examined using the Pd/P<sup>l</sup>Bu<sub>3</sub> catalytic system (Table 2). All starting bromoarenes were obtained in 2–5 steps in good overall yields from commercially available 2-substituted bromoarenes using standard chemistry (see Supporting Information). The most generally applicable conditions were found with Pd(OAc)<sub>2</sub> (10 mol%) as palladium source in combination to (*t*-Bu<sub>3</sub>PH)BF<sub>4</sub> (20 mol%) in DMF at 140 °C. On a multigram scale, the amounts of palladium and phosphonium were routinely decreased to 6 mol% and 12 mol%, respectively, without significant impact on the yield. As shown in Table 2, the C–H activation reaction showed a good tolerance to a variety of substituents on the aromatic or 4-membered ring. As only major limitation, we found it was restricted to substrates bearing a quaternary benzylic carbon, as the reaction of bromobenzene **1b** bearing a tertiary benzylic carbon (entry 2) failed to produce the corresponding BCB. In this case a mixture of products including the proto-debrominated product (major) and the styrene arising from β-H elimination (minor)<sup>6n,7</sup> were

observed. This limitation was overcome in an indirect manner using diester-type substrates and decarboxylation, as will be shown later.

We next examined the reaction of bromobenzenes bearing different substituents on the benzylic carbon (entries 3–13). First, the presence of a functional group was not absolutely required, since the reaction worked on 2-bromo-*tert*-butylbenzene **1c** (entry 3). The isolated yield was only 46% but this was due to the volatility of BCB **2c** that was the only observed product. This result stands in sharp contrast to the production of a dimeric BCB in the seminal work of Dyker starting from 2-iodo-*tert*-butylbenzene.<sup>6c</sup> This dimer was never observed under our conditions. This probably reflects the influence of the phosphine ligand on the outcome of the reaction (see mechanistic considerations). The avoidance of the production of oligomers renders this process particularly predictable and synthetically useful for the synthesis of BCB. A *tert*-butyl ester (entry 4) and other heteroatom-containing functional groups (entries 5–8) were tolerated on the benzylic position. However alcohols (entries 5–6) and amines (entry 7) had to be protected to avoid side reactions such as intramolecular C–N or C–O coupling. Importantly, the reaction was not restricted to *gem*-dimethyl substrates (entries 6, 9–12). In particular, the C–H activation proved remarkably regioselective with substrates bearing one methyl group and another alkyl group (entries 9–11). No sign of C–H activation on the other alkyl group, which would have given rise to the corresponding olefin by β-H elimination,<sup>7b</sup> was observed. This shows the strong steric preference for C–H activation at benzylic methyl groups.<sup>6l</sup> In addition, no intramolecular Mizoroki-Heck coupling was observed when a terminal olefin was present on the alkyl chain (entry 10), provided there was a sufficiently long spacer (four methylenes) between the olefin and the benzylic carbon. With shorter spacers (three methylenes or less), intramolecular carbopalladation became predominant. Starting from diesters **11–m** (entries 12–13), the corresponding BCB **2l–m** were again produced in good yield. This provides an indirect entry into BCB containing a tertiary benzylic carbon, that could not be obtained directly by C–H activation (entry 2). Indeed BCB **2l–m** could be both decarboxylated (Scheme 2), either from **2l** using a Krapcho-type procedure to yield carboxylic acid **4**,<sup>15</sup> or from **2m** by TFA-mediated cleavage of the *t*-butyl ester and thermal decarboxylation of the corresponding carboxylic acid to yield methyl ester **5**.<sup>16</sup>

The C–H activation of bromoarenes containing various aryl substituents was next examined (Table 2, entries 14–28). First, substrates bearing a substituent *para* to the quaternary benzylic carbon were reacted under the usual conditions (entries 14–20), to give the corresponding BCB in moderate to good yields regardless of their electron-withdrawing or donating nature. Remarkably, pyridine **1t** also underwent C–H activation to give pyridocyclobutene **2t** in 62% yield (entry 20). This constitutes a new entry to this synthetically useful motif that is otherwise obtained by [2 + 2] cycloaddition of a pyridyne and a ketene acetal.<sup>17</sup> Next, the C–H activation of bromobenzenes bearing a substituent *para* to the bromine atom was studied (entries 21–27). Surprisingly, the reaction of *p*-fluorobromobenzene **1u** gave an inseparable mixture of two BCB regioisomers **2u** and

(12) (a) Nishiyama, M.; Yamamoto, T.; Koie, Y. *Tetrahedron Lett.* **1998**, 39, 617. (b) Littke, A. F.; Fu, G. C. *Angew. Chem., Int. Ed.* **1998**, 37, 3387. (c) Aranyos, A.; Old, D. W.; Kiyomori, A.; Wolfe, J. P.; Sadighi, J. P.; Buchwald, S. L. *J. Am. Chem. Soc.* **1999**, 121, 4369. (d) Kataoka, N.; Shelby, Q.; Stambuli, J. P.; Hartwig, J. F. *J. Org. Chem.* **2002**, 67, 5553. (e) Christmann, U.; Vilar, R. *Angew. Chem., Int. Ed.* **2005**, 44, 366.

(13) Netherton, M. R.; Fu, G. C. *Org. Lett.* **2001**, 3, 4295.

(14) On this scale the Pd<sub>2</sub>dba<sub>3</sub>/*t*-Bu<sub>3</sub>PH)BF<sub>4</sub> combination is economically advantageous and at this temperature using 10 mol% palladium(0) was necessary to ensure a reproducible yield.

(15) Evans, P. A.; Kennedy, L. J. *J. Am. Chem. Soc.* **2001**, 123, 1234.

(16) Oppolzer, W. A.; Bättig, K.; Petrzilka, M. *Helv. Chim. Acta* **1978**, 61, 1945.

(17) Mariet, N.; Ibrahim-Ouali, M.; Santelli, M. *Tetrahedron Lett.* **2002**, 43, 5789.

Table 2. Scope of the synthesis of BCB by C(sp<sup>3</sup>)-H<sup>a</sup>

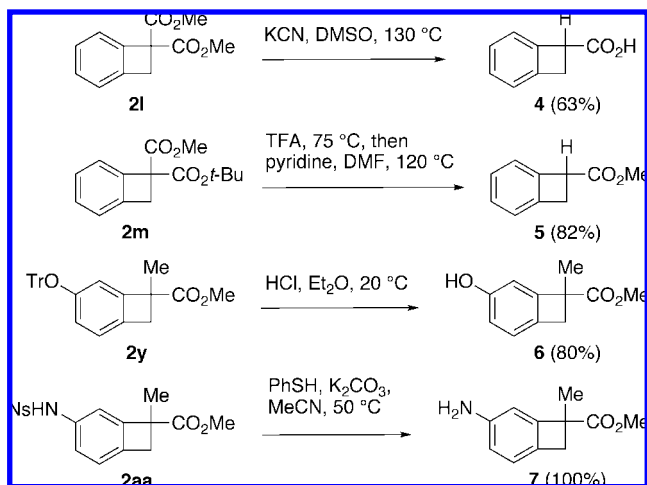
entry	bromoarene	BCB product(s) <sup>b</sup>	time (min)	yield (%) <sup>c</sup>	entry	bromoarene	BCB product(s) <sup>b</sup>	time (min)	yield (%) <sup>c</sup>
1			60	78	15			75	92
2		-	>240	0	16			45	51
3			60	46	17			45	74
4			45	68	18			60	78
5			90	69	19			60	87
6			60	58	20			60	62
7 <sup>d</sup>			60	85	21			70	68
8			70	58	22			80	81
9			50	75	23			150	74
10			60	77	24			60	83
11			60	72	25 <sup>e</sup>			60	70
12			60	71	26			90	44 <sup>f</sup>
13			80	70	27 <sup>g</sup>			60	72
14			60	63	28			90	60

<sup>a</sup> Reaction conditions: Pd(OAc)<sub>2</sub> (10 mol%), (t-Bu<sub>3</sub>PH)BF<sub>4</sub> (20 mol%), K<sub>2</sub>CO<sub>3</sub> (1.3 equiv), DMF, 140 °C. <sup>b</sup> The ratio of regioisomers (when applicable) was measured by <sup>1</sup>H NMR and GC. <sup>c</sup> Yields of isolated products. <sup>d</sup> Ts = tosyl. <sup>e</sup> Tr = triphenylmethyl. <sup>f</sup> Yield after recrystallization. <sup>g</sup> Ns = 4-nitrophenylsulfonyl.

**3u** (entry 21), that were clearly identified by NMR analysis. This phenomenon, that gives invaluable information on the

reaction mechanism (vide infra), was never described before to our knowledge.<sup>6</sup> Increasing the steric bulk with the replacement

Scheme 2. Reactions of BCB Obtained by C–H Activation



of the fluorine atom by a trifluoromethyl group (entry 22) suppressed the production of the “abnormal” regioisomer, and BCB **2v** was formed as sole product. The same trend was observed with an oxygenated substituent: the reaction of *p*-methoxybromobenzene **1w** gave a *ca.* 10:1 mixture of inseparable BCB regioisomers **2w** and **3w** (entry 23). Dimethoxybromobenzene **1x** (entry 24) gave rise to BCB regioisomers **2x** and **3x** in a similar ratio. To suppress the formation of the “abnormal” regioisomer in this series of oxygenated molecules, substrate **1y** containing a bulkier trityl ether was prepared (entry 25). As expected, the C–H activation reaction of **1y** furnished BCB **2y** as the sole observable regioisomer, in 70% isolated yield. The trityl group of **2y** can be removed by treatment with HCl in diethyl ether to give phenol **6** in 80% yield (Scheme 2). The reaction of diester **1z** (entry 26) gave rise to the corresponding BCB **2z** in 44% yield after recrystallization to remove undesired byproduct (including the abnormal regioisomer and decarboxylation products). The three-dimensional structure of **2z** was deduced from X-ray diffraction analysis (Figure 2), which shows the characteristic distortion of the quaternary carbon-containing cyclobutene ring. The reaction of nosyl-protected *p*-aminobromobenzene **1aa** furnished BCB **2aa** in 72% yield, with no observable trace of regioisomer (entry 27). Again this result is noteworthy since it is notorious that amino substituents are not compatible with most methods used to form the 4-membered ring of BCB. The nosyl group of **2aa** was cleaved easily as described by Fukuyama et al.<sup>18</sup> to give the corresponding aniline **7** quantitatively (Scheme 2). Finally, the reaction of chlorobromobenzene **1ab** furnished BCB **2ab** in satisfying yield (entry 28), which shows the lack of reactivity of the C–Cl bond at this position of the aromatic ring under these reaction conditions. All synthesized BCB showed good stability under the reaction conditions and upon storage. This property can be imputed to the presence of the quaternary benzylic carbon and the absence of a strong electron-donating substituent directly on the cyclobutene ring, that both disfavor electrocyclic ring-opening and thus the production of the reactive *ortho*-xylylene form.<sup>10,11</sup>

**3. Computational Studies.** The synthesis of Pd-catalyzed benzocyclobutene described in this work is highly dependent on the nature of the base, the phosphine ligand and the solvent

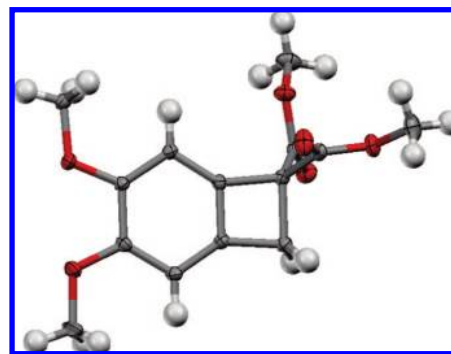


Figure 2. X-ray Crystal Structure of BCB **2z** (30% probability ellipsoids plot).

(Table 1). Moreover, reactions on substituted aromatic rings evidenced the occurrence of an isomerization process during the catalytic cycle (Table 2, compounds **3**). To shed more light on these observations, a computational study of the catalytic cycle was carried out at the DFT level with the hybrid functional B3PW91 (see Supporting Information for computational details). There are many parameters to take into account but the focus of the theoretical study is (i) to delineate the basic features of the mechanism, (ii) to study the influence of the nature of the base, and (iii) to explain the origin of the isomerization process observed with the substituted aromatic rings.

The basic features of the mechanism were studied on the model system 2-bromo-*tert*-butylbenzene **1c** and Pd(P<sup>*t*</sup>Bu<sub>3</sub>). Bromoarene **1c** was selected as it was shown to react experimentally and lacks any influence of a functional group close to the activated methyl. The phosphine considered was P<sup>*t*</sup>Bu<sub>3</sub> as it was shown to be the most efficient and it allows to exclude a mechanism involving two phosphines coordinated at Pd.<sup>6g,12c,19</sup> The mechanism of base-assisted cyclometalation has been studied computationally by several groups showing the critical influence of coordination of the base to the metal to achieve the C–H activation.<sup>6l,20</sup> Experimentally, it was shown that carbonate is the most efficient base, bicarbonate was shown to be slightly less active and the activity with acetate was significantly lower (Table 1, entries 1, 5, 10). Generally, even though the experimental results are often better with carbonate, the computational studies already published considered either bicarbonate,<sup>20c,e–g</sup> or acetate<sup>6l,20h</sup> as a model for the base. In the present work, the three different bases have been considered to study their influence on the C–H activation. To take into account the charged species involved in the mechanism, the geometries were determined in the gas phase at the B3PW91 level but the energies were evaluated including a continuum to model the solvent according to the PCM procedure. The solvent

(18) Fukuyama, T.; Jow, C.-K.; Cheung, M. *Tetrahedron Lett.* **1995**, *36*, 6373.

(19) (a) Stambuli, J. P.; Bühl, M.; Hartwig, J. F. *J. Am. Chem. Soc.* **2002**, *124*, 9346. (b) Stambuli, J. P.; Incarvito, C. D.; Bühl, M.; Hartwig, J. F. *J. Am. Chem. Soc.* **2004**, *126*, 1184. (c) Ikawa, T.; Barder, T. E.; Biscoe, M. R.; Buchwald, S. L. *J. Am. Chem. Soc.* **2007**, *129*, 13001. (20) (a) Biswas, B.; Sugimoto, M.; Sakaki, S. *Organometallics* **2000**, *19*, 3895. (b) Davies, D. L.; Donald, S. M. A.; Macgregor, S. A. *J. Am. Chem. Soc.* **2005**, *127*, 13754. (c) García-Cuadrado, D.; Braga, A. A. C.; Maseras, F.; Echavarren, A. M. *J. Am. Chem. Soc.* **2006**, *128*, 1066. (d) Alonso, I.; Alcamí, M.; Mauleón, P.; Carretero, J. C. *Chem.–Eur. J.* **2006**, *12*, 4576. (e) García-Cuadrado, D.; de Mendoza, P.; Braga, A. A. C.; Maseras, F.; Echavarren, A. M. *J. Am. Chem. Soc.* **2007**, *129*, 6880. (f) Özdemir, I.; Demir, S.; Çetinkaya, B.; Gourlaouen, C.; Maseras, F.; Bruneau, C.; Dixneuf, P. H. *J. Am. Chem. Soc.* **2008**, *130*, 1156. (g) Lafrance, M.; Rowley, C. N.; Woo, T. K.; Fagnou, K. *J. Am. Chem. Soc.* **2006**, *128*, 8754. (h) Gorelsky, S. I.; Lapointe, D.; Fagnou, K. *J. Am. Chem. Soc.* **2008**, *130*, 10848.

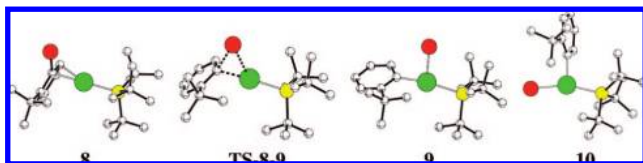


**Figure 3.** Optimized geometries for the extrema located along the pathway for C–Br oxidative addition of **1c** to Pd(P<sup>t</sup>Bu<sub>3</sub>). H atoms have been omitted for clarity.

giving the best results experimentally, DMF, was selected and the parameters used are those of Stassen and co-workers.<sup>21</sup> In the remaining of the paper, only PCM energies on gas phase optimized geometries are given.

**3.1. C–Br Oxidative Addition.** The oxidative addition of aryl-halide bond to Pd<sup>0</sup> has been extensively studied computationally as it is the first step in any Pd-catalyzed cross-coupling reaction.<sup>22</sup> C–Br activation is generally considered to proceed through oxidative addition from an η<sup>2</sup>-C=C complex of bromobenzene. In the case of iodobenzene, an alternative mechanism with direct I⋯Pd interaction has been proposed by Thiel et al.<sup>22g</sup> However this mechanism is operating when two phosphine ligands are present on Pd, which is not the case with P<sup>t</sup>Bu<sub>3</sub>. Therefore only the oxidative addition pathway has been considered. Figure 3 shows the geometry of the various extrema located along the pathway for C–Br bond cleavage. The η<sup>2</sup>-C=C complex **8** is easily obtained with a formation energy of –67.2 kJ mol<sup>–1</sup>. The activation barrier to reach **TS-8-9**, 19.7 kJ mol<sup>–1</sup>, is low and very similar to that obtained by Lin (22.6 kJ mol<sup>–1</sup>) for Ph–Br reacting with Pd(PMe<sub>3</sub>),<sup>22h</sup> and lower than that obtained by Ahlquist and Norrby (36.7 kJ mol<sup>–1</sup>) for Ph–Cl reacting with Pd(P<sup>t</sup>Bu<sub>3</sub>).<sup>22k</sup> In the transition state **TS-8-9**, the C–Br bond is longer than in **8** (1.962 Å, **8**; 2.161 Å, **TS-8-9**) and the Pd–C bond is shorter (2.130 Å, **8**; 2.019 Å, **TS-8-9**) in agreement with an oxidative addition process.

The product of C–Br activation, **9**, is different from the X-ray structure obtained by Hartwig et al. on Pd(Ph)(Br)(P<sup>t</sup>Bu<sub>3</sub>).<sup>19b</sup> In the latter compound, the aryl is *trans* to the vacant site with the phenyl ring perpendicular to the plane, whereas the Br atom is *trans* to the phosphine. A structure similar to that observed by Hartwig, **10** (Figure 3), was found to be 27.2 kJ mol<sup>–1</sup> more stable than **9**. In both structures **9** and **10**, contrary to the complex of Hartwig, there was no clear indication of any agostic interaction developing between a C–H bond on a <sup>t</sup>Bu group (phosphine or aryl) and the palladium center. The C–Br oxidative addition reaction is exothermic with a reaction energy of –34.5 kJ mol<sup>–1</sup> to form **9** from **8**. The reaction energy for Ph–Br reacting with Pd(PMe<sub>3</sub>) was computed by Lin et al. to be –14.2 kJ mol<sup>–1</sup>.<sup>22h</sup> The larger exothermicity in our case could be explained by a greater stabilization of Pd<sup>II</sup> by the more

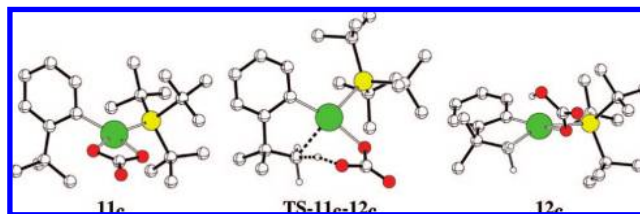


**Figure 4.** Optimized geometry for the extrema located along the pathway for C–H activation by the coordinated carbonate after Br<sup>–</sup> substitution in **10**. H atoms not involved in the process have been omitted for clarity.

**Scheme 3.** Reaction Energies (kJ mol<sup>–1</sup>) for the Substitution Reaction of Br<sup>–</sup> by the Various Bases KO<sub>2</sub>CX in **10** (Δ<sub>1</sub>E<sub>Y</sub>) and **9** (Δ<sub>c</sub>E<sub>Y</sub>)

<b>10</b> + KO <sub>2</sub> CX	→	<b>11<sub>Y</sub></b> + KBr	<b>9</b> + KO <sub>2</sub> CX	→	<b>13<sub>Y</sub></b> + KBr
		Δ <sub>1</sub> E <sub>Y</sub>			Δ <sub>c</sub> E <sub>Y</sub>
X = Me, Y = A		-51.4			-17.2
X = OH, Y = B		-41.6			-6.6
X = O <sup>–</sup> , Y = C		-136.6			-40.8

electron-rich phosphine P<sup>t</sup>Bu<sub>3</sub>. The C–Br oxidative addition is thus an easy process with a low activation barrier and a significant negative reaction energy. Two isomers are possible for the resulting Pd<sup>II</sup> ML<sub>3</sub> complex, **9** and **10**, with the isomer featuring the vacant site *trans* to the aryl ligand, **10**, being more stable.

**3.2. C–H Activation from 10.** Several computational studies have shown how proton abstraction from an aromatic C(sp<sup>2</sup>)-H bond is made easier upon coordination of the base *trans* to the aryl ring.<sup>20</sup> Recently, C(sp<sup>3</sup>)-H activation has also been addressed computationally.<sup>61</sup> In some instances this intramolecular pathway has been compared with an intermolecular pathway where the base is not coordinated to the metal.<sup>20e,23</sup> For Pd-complexes with a bidentate phosphine, it was shown experimentally and computationally that an intermolecular pathway is preferred.<sup>23</sup> The C–H activation can even be performed by the coordinated Br in the case of electron-deficient arenes as shown by Fagnou.<sup>20g</sup> Nevertheless, in the majority of the cases the preferred pathway is the intramolecular with coordination of the base. The only geometry considered in these computational studies for the Pd(Ar)(PR<sub>3</sub>) complexes is with the phosphine *cis* to the aromatic ring, leaving thus two *cis*-vacant sites for the base to interact with Pd.<sup>61,20c,e,g</sup>

Following these works, substitution of Br<sup>–</sup> in **10** by the various bases studied yielded (κ<sup>2</sup>-O<sub>2</sub>CX) Pd complexes, **11<sub>Y</sub>** (X = Me, acetate, Y = A; X = OH, bicarbonate, Y = B; X = O<sup>–</sup>, carbonate, Y = C, see Figure 4 for geometry of **11c**). The complexes with acetate, **11<sub>A</sub>**, and bicarbonate, **11<sub>B</sub>**, are neutral and the complex with carbonate, **11<sub>C</sub>**, is anionic. The energy of the reaction Δ<sub>1</sub>E<sub>Y</sub> is computed to be negative for all cases (Scheme 3). The reaction is more exothermic in the case of carbonate because the dianionic nature of the base allows a more efficient (κ<sup>2</sup>-O<sub>2</sub>CX) bonding interaction.

From these complexes, C–H activation is effective through **TS-11<sub>Y</sub>-12<sub>Y</sub>** (see Figure 4 for geometry of **TS-11c-12c**). The geometry of these TS is very similar to that obtained in other computational studies. However, the activation barriers are significantly higher than those reported in the literature (Table

(21) Böes, E. S.; Livotto, P. R.; Stassen, H. *Chem. Phys.* **2006**, *331*, 142.

(22) (a) Bickelhaupt, F. M.; Ziegler, T.; von Schleyer, P. R. *Organometallics* **1995**, *14*, 2288. (b) Diefenbach, A.; Bickelhaupt, F. M. *J. Chem. Phys.* **2001**, *5*, 4030. (c) Albert, K.; Gisdakis, P.; Rösch, N. *Organometallics* **1998**, *17*, 1608. (d) Jakt, M.; Johannissen, L.; Rzepa, H. S.; Widdowson, D. A.; Wilhelm, R. *J. Chem. Soc., Perkin Trans. 2* **2002**, 576. (e) Sundermann, A.; Uzan, O.; Martin, J. M. L. *Chem.–Eur. J.* **2001**, *7*, 1703. (f) Senn, H. M.; Ziegler, T. *Organometallics* **2004**, *23*, 2980. (g) Gooßen, L. J.; Koley, D.; Hermann, H.; Thiel, W. *Chem. Commun.* **2004**, 2141. (h) Lam, K. C.; Marder, T. B.; Lin, Z. *Organometallics* **2007**, *26*, 758. (i) Goossen, L. J.; Koley, D.; Hermann, H. L.; Thiel, W. *Organometallics* **2005**, *24*, 2398. (j) Ahlquist, M.; Frstrup, P.; Tanner, D.; Norrby, P.-O. *Organometallics* **2006**, *25*, 2066. (k) Ahlquist, M.; Norrby, P.-O. *Organometallics* **2007**, *26*, 550.

(23) Pascual, S.; de Mendoza, P.; Braga, A. A. C.; Maseras, F.; Echavarren, A. M. *Tetrahedron* **2008**, *64*, 6021.

**Table 3.** Activation Energy,  $\Delta E^\ddagger$ , and Reaction Energy,  $\Delta E$  ( $\text{kJ mol}^{-1}$ ) for the C–H Activation Process by the Coordinated Base in **11<sub>Y</sub>** and **13<sub>Y</sub>** (Y = A, Acetate; Y = B, Bicarbonate; Y = C, Carbonate)

	<b>11<sub>Y</sub></b>		<b>13<sub>Y</sub></b>	
	$\Delta E^\ddagger$	$\Delta E$	$\Delta E^\ddagger$	$\Delta E$
Y = A	138.0	85.0	122.3	−19.0
Y = B	143.5	100.1	118.3	−6.8
Y = C	187.9	78.8	115.3	−82.5

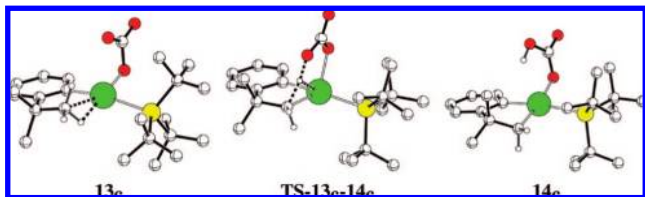


**Figure 5.** Optimized geometry for the extrema located along the pathway for C–H activation by the coordinated carbonate after  $\text{Br}^-$  substitution in **9**. H atoms not involved in the process have been omitted for clarity.

3). For  $\text{C}(\text{sp}^2)\text{-H}$  activation by  $\text{HCO}_3^-$ , Maseras, Echavarren et al. reported an activation barrier of  $98.4 \text{ kJ mol}^{-1}$ .<sup>20c,e,23</sup> The present activation barrier with bicarbonate is significantly higher ( $143.5 \text{ kJ mol}^{-1}$ ) reflecting both the lower acidity of  $\text{C}(\text{sp}^3)\text{-H}$  bonds and the increased steric bulk of the phosphine ( $\text{PH}_3$  was the model phosphine in the study by Maseras). The importance of the bulk of the phosphine is illustrated by a comparison with a study by Fagnou.<sup>61</sup> In this case,  $\text{C}(\text{sp}^3)\text{-H}$  activation was studied with  $\text{AcO}^-$  as base and  $\text{PMe}_3$  as phosphine. The computed activation barrier ( $113 \text{ kJ mol}^{-1}$ ) is again lower than the value obtained in the present work ( $138 \text{ kJ mol}^{-1}$ ). Thus, in the present system with  $\text{P}^t\text{Bu}_3$  *cis* to the aromatic ring and a  $\text{C}(\text{sp}^3)\text{-H}$  bond to cleave, the computed activation barrier are significantly higher than in other computational studies. The value obtained for  $\text{CO}_3^{2-}$  reaches a high  $187.9 \text{ kJ mol}^{-1}$ . This is a consequence of the necessity to break the very stable ( $\kappa^2\text{-O}_2\text{CX}$ ) interaction in **11<sub>C</sub>**.

The trends in the computed barrier (Table 3) are completely opposite to the experimental results (Table 1). Carbonate is the worst base and acetate is the best. Moreover the C–H activation reaction is in all cases strongly endothermic with reaction energies greater than  $80 \text{ kJ mol}^{-1}$  (Table 3). This is the result of creating a  $\text{Pd}\text{-C}(\text{sp}^3)$  bond *trans* to P and losing the ( $\kappa^2\text{-O}_2\text{CX}$ ) coordination of the base. As a matter of fact, in the case of carbonate, the  $\text{Pd}\text{-P}$  bond distance elongates by  $0.05 \text{ \AA}$  in the TS ( $2.351 \text{ \AA}$ , **11<sub>C</sub>**;  $2.402 \text{ \AA}$ , **TS-11<sub>C</sub>-12<sub>C</sub>**), but the elongation reaches a high  $0.3 \text{ \AA}$  in the product ( $2.685 \text{ \AA}$ , **12<sub>C</sub>**). There is thus significant loss of  $\text{Pd}\text{-PR}_3$  interaction in the product of C–H activation, leading to a strongly endothermic transformation. The energetic pattern is thus very unfavorable and the C–H activation of the *t*Bu group is not likely to proceed from coordination of the base to **10**.

**3.3. C–H Activation from 9.** The actual product of C–Br activation is not the more stable compound **10** but complex **9** featuring a bromide *trans* to the vacant site. Substitution in this complex of  $\text{Br}^-$  for the various bases yielded the three ( $\kappa^1\text{-O}_2\text{CX}$ ) complexes **13<sub>Y</sub>** (X = Me, acetate, Y = A; X = OH, bicarbonate, Y = B; X =  $\text{O}^-$ , carbonate, Y = C, see Figure 5 for geometry of **13<sub>C</sub>**). The substitution reaction  $\Delta_c E_Y$  is exothermic (Scheme 3) but the thermodynamic preference for the ( $\kappa^1\text{-O}_2\text{CX}$ ) bonding in **13<sub>Y</sub>** is less strong than for the ( $\kappa^2\text{-O}_2\text{CX}$ ) bonding in **11<sub>Y</sub>**. Substitution by acetate or bicarbonate

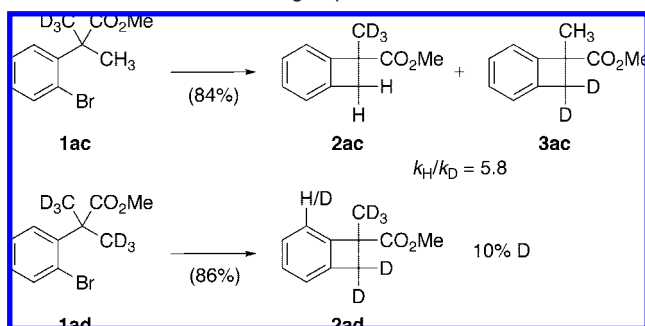
is only slightly favored, whereas coordination of carbonate is likely to displace  $\text{Br}^-$ .

Contrary to the bromo complex **9**, complexes **13<sub>Y</sub>** feature a clear agostic interaction of one C–H bond of the *t*Bu group on the aromatic ring (see Figure 5 for **13<sub>C</sub>**,  $\text{Pd}\cdots\text{C} = 2.436 \text{ \AA}$ ,  $\text{Pd}\cdots\text{H} = 1.878 \text{ \AA}$ ,  $\text{C}\text{-H} = 1.135 \text{ \AA}$ ). The proton transfer from  $\text{C}(\text{sp}^3)$  to O is effective in a plane perpendicular to the  $\text{P}\text{-Pd}\text{-Ph}$  axis as illustrated in the geometry of **TS-13<sub>C</sub>-14<sub>C</sub>** shown in Figure 5. The agostic  $\text{Pd}\cdots\text{C}$  bond distance has been reduced by ca.  $0.1 \text{ \AA}$  ( $2.350 \text{ \AA}$ , **TS-13<sub>C</sub>-14<sub>C</sub>**;  $2.436 \text{ \AA}$ , **13<sub>C</sub>**), the C–H bond is elongated to  $1.4 \text{ \AA}$  and the  $\text{H}\cdots\text{O}$  distance has decreased to  $1.3 \text{ \AA}$ , while the  $\text{Pd}\cdots\text{H}$  bond is still long ( $2.024 \text{ \AA}$ ), speaking against any direct  $\text{Pd}\cdots\text{H}$  bonding in the TS. The reaction is best described as a proton transfer to the basic uncoordinated oxygen atom of the carbonate. Table 3 shows a comparison of the activation barriers and the reaction energies for the transformation for the three different bases. The activation barriers are all lower than the corresponding value obtained for the C–H activation from the ( $\kappa^2\text{-O}_2\text{CX}$ ) complexes **11<sub>Y</sub>**, only slightly for acetate (Y = A) and bicarbonate (Y = B) but significantly for carbonate (Y = C). As a result the activation barrier is computed to be the lowest for carbonate, in agreement with the experimental results. The differences in magnitude between the computed activation barriers qualitatively reproduce the difference in activity (3:1 for carbonate vs bicarbonate and 7.3:1 for carbonate vs acetate). This is in qualitative agreement with the conversions observed experimentally (Table 1, entries 1, 5, 10), albeit on a different system (**1a**).

Contrary to the case of **11<sub>Y</sub>**, the C–H activation in **13<sub>Y</sub>** is computed to be exothermic (Table 3). As the phosphine ligand is already *trans* to the strongest  $\sigma$ -donor (aryl), there is no particular energetic penalty introduced on the  $\text{Pd}\text{-PR}_3$  interaction in the C–H activation. The  $\text{Pd}\cdots\text{P}$  bond distance is in fact identical in the reactant **13<sub>C</sub>** ( $2.532 \text{ \AA}$ ) and in the product **14<sub>C</sub>** ( $2.542 \text{ \AA}$ ) and even slightly shorter in **TS-13<sub>C</sub>-14<sub>C</sub>** ( $2.450 \text{ \AA}$ ). The forming  $\text{Pd}\text{-C}(\text{sp}^3)$  bond is *trans* to the coordinated oxygen of the base. In the cases of acetate and bicarbonate, the proton transfer is accompanied by a switch of the nature of the coordinated oxygen from alkoxy in **13<sub>Y</sub>** ( $\text{Pd}\text{-O} = 2.057 \text{ \AA}$ , Y = A;  $2.051 \text{ \AA}$ , Y = B) to ketone in **14<sub>Y</sub>** ( $\text{Pd}\text{-O} = 2.365 \text{ \AA}$ , Y = A;  $2.399 \text{ \AA}$ , Y = B). The loss of  $\text{Pd}\text{-O}$  interaction is compensated by the energy gain of creating the O–H bond. In the case of the carbonate, the  $\text{Pd}\text{-O}$  bond distance only elongates by  $0.15 \text{ \AA}$  upon going from **13<sub>C</sub>** to **14<sub>C</sub>** ( $1.99$  vs  $2.148 \text{ \AA}$ ) as result of the “dianionic” nature of the carbonate. There is no need for extensive reorganization of the electronic structure of the base to achieve the proton transfer. As a consequence the activation barrier is lower and the reaction is more exothermic (Table 3).

For the C–H activation step in the presence of a bulky phosphine there is thus a clear preference for a pathway with  $\kappa^1$ -coordination of the base *cis* both to the aromatic ring and to the phosphine (Table 3). The substitution of  $\text{Br}^-$  by the base is computed to be an exothermic process with a larger thermodynamic driving force for carbonate (Scheme 3). The activation barrier computed with the various bases are similar in magnitude but with a slightly lower value for carbonate as observed experimentally. The lower activation barrier and the more exothermic reaction energy (Table 3) for the proton transfer in **13<sub>C</sub>** are due to the ease for carbonate to reorganize its electronic structure both to achieve good interaction with Pd through one oxygen atom and to develop good basic properties through the other oxygen atom during the whole process.



Scheme 4. Deuterium-Labeling Experiments<sup>a</sup>

<sup>a</sup> Reactions conditions: see Table 2.

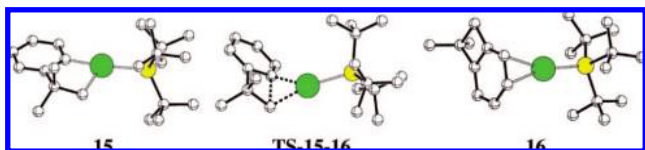


**Figure 6.** Optimized geometry for the extrema located along the pathway for C–C coupling from **15**. H atoms have been omitted for clarity.

**3.4. C–C Reductive Coupling.** The C–H activation step is always considered to be the rate-limiting step as confirmed by experimental values for kinetic isotope effect usually larger than 3. However, generally, the C–C coupling step does not involve the creation of a constrained 4-membered ring. It was thus important to check if the C–H activation step remains the rate-determining step in the present case.

The reaction of partially deuterated substrate **1ac** under the reoptimized conditions (Table 2) allowed the determination of a primary intramolecular isotope effect of 5.8 (Scheme 4), that was similar to those reported in the literature for similar types of reactions.<sup>61,20c,e,23</sup> This value is in agreement with C–H activation being the rate-limiting step.

All attempts to locate a transition state for C–C coupling with the protonated base still coordinated failed. Dissociation of the protonated base from **14<sub>V</sub>** yielded the complex **15** (Figure 6) featuring a vacant site trans to the alkyl group. The dissociation is endothermic but the binding energy of HO<sub>2</sub>CX is low (20.5 kJ mol<sup>-1</sup>, X = CH<sub>3</sub>; 7.4 kJ mol<sup>-1</sup>, X = OH; 21.0 kJ mol<sup>-1</sup>, X = O<sup>-</sup>), therefore entropy effects associated to the dissociation will override the enthalpy contributions and will drive the reaction toward **15**.

The transition state for C–C coupling from **15** has been located on the potential energy surface (Figure 6) and the activation barrier amounts to 94 kJ mol<sup>-1</sup>. In the transition state, the forming C···C bond distance is 1.893 Å, while the Pd···C bond distances are 2.079 Å (aryl) and 2.174 Å (alkyl). The product of the reaction, **16**, is a  $\pi$ -complex of the aromatic ring (Figure 6) and the transformation from **15** to **16** is exothermic (–15.7 kJ mol<sup>-1</sup>). The coordination energy of the benzocyclobutene **2c** to Pd(P<sup>t</sup>Bu<sub>3</sub>) amounts to –79.1 kJ mol<sup>-1</sup>, a quantity similar to the binding energy of **1c** (–67.2 kJ mol<sup>-1</sup>). Therefore the catalyst Pd(P<sup>t</sup>Bu<sub>3</sub>) will be easily regenerated by dissociation of **2c** to enter a new catalytic cycle upon coordination of **1c**. The C–C coupling step is thus easier than the C–H activation step, even in the case of the formation of the 4-membered ring. The highest energy barrier along the catalytic cycle is thus that corresponding to the C–H activation step. For this step the nature of the base has an influence and it was shown that the height of the barrier varies as CO<sub>3</sub><sup>2-</sup> < HCO<sub>3</sub><sup>-</sup> < AcO<sup>-</sup> in qualitative agreement with the experimental results.

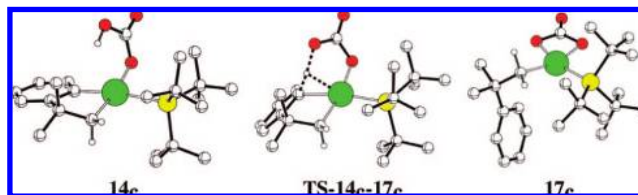


**Figure 7.** Optimized geometry for the extrema located along the pathway for proton transfer to the aromatic ring from **14<sub>C</sub>**. H atoms not involved in the process have been omitted for clarity.

**3.5. 1,4-Migration of Palladium.** With bromoarenes bearing a substituent *para* to Br, the regioisomeric product **3** resulting formally to a 1,4-migration of Pd has been observed in some instances together with the expected product **2** (Table 2, entries 21, 23, 24). The 1,4-palladium migration was also evidenced experimentally using deuterated substrate **1ad** (Scheme 4). Partial incorporation of deuterium (10%) was indeed observed on the *ortho* aromatic position by <sup>2</sup>H NMR.<sup>24</sup> The observation of regioisomers **3** and the partial incorporation of D in product **2ad** implies that a hydrogen, initially on the alkyl group, ends up on the aromatic ring. From the product of C–H activation, **14<sub>C</sub>**, a transition state, TS-14<sub>C</sub>-17<sub>C</sub>, for proton transfer to the aromatic ring has been located on the potential energy surface (Figure 7). The activation barrier is computed to be 81.9 kJ mol<sup>-1</sup> and the reaction is moderately exothermic (–27.8 kJ mol<sup>-1</sup>) to form the  $\kappa^2$ -carbonate complex **17<sub>C</sub>**. Thus the proton transfer to form **17<sub>C</sub>** is competitive with the dissociation of HCO<sub>3</sub><sup>-</sup> from **14<sub>C</sub>** to form **15** and then to form **2c** through C–C coupling. In fact the activation barrier for protonation of the aromatic ring is lower than the one for C–C reductive elimination (94 kJ mol<sup>-1</sup>). Thus formation of **17<sub>C</sub>** en route to forming **2c** would explain the experimental observations. Indeed rotation of the aromatic ring in **17<sub>C</sub>** gives access to a proton transfer from the other *ortho* position to reform **14<sub>C</sub>** that would ultimately give the benzocyclobutene resulting from 1,4-palladium migration. This process is similar to the hydrogen shifts studied computationally by Dedieu et al.<sup>25</sup> However in their case the migration was effective through interaction with the Pd center. In the present case the coordinated base is responsible for the proton migration. 1,4-Migrations of palladium were observed experimentally in many instances,<sup>6g,9,26,27</sup> but their exact mechanism has remained elusive. The present work suggests that Pd-bound carbonate plays a key role as proton shuttle in these migration processes.

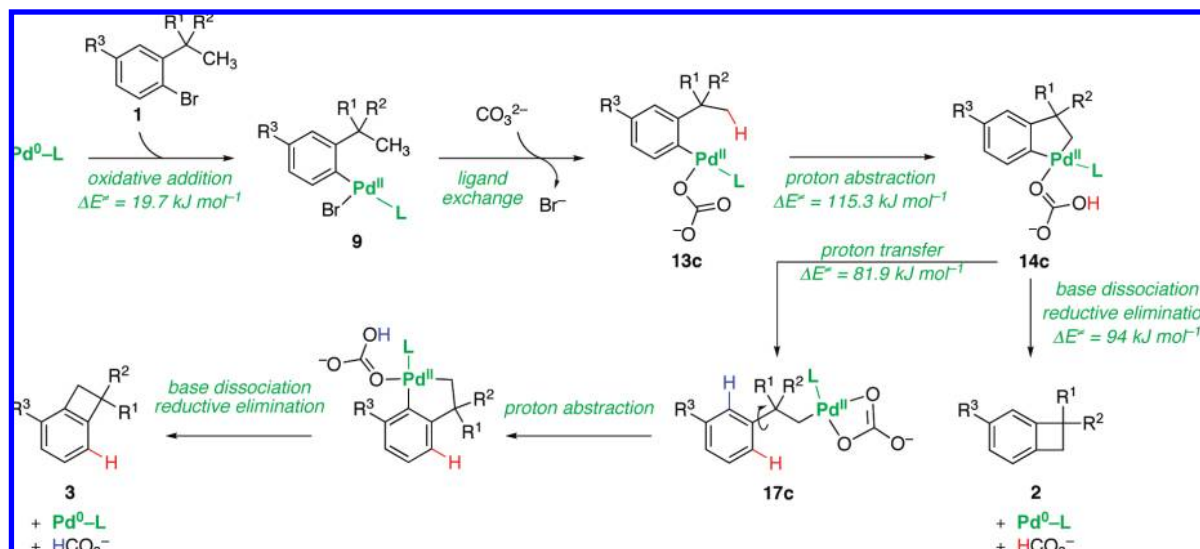
The above transformation not only explains the regioisomers observed experimentally, but it is also a strong support for the

(24) The low level of incorporation, compared to the amount of “abnormal” regioisomer observed with substituents *para* to the bromine and in particular with fluorine (Table 2, entry 21), might reflect a tendency of electron-withdrawing substituents to favour the **17<sub>C</sub>** → **3** pathway: see refs 20c, e, and 23. Alternatively, an intermolecular H/D exchange with traces of water or another protic source could be operating: see ref 26e.

(25) (a) Mota, A. J.; Dedieu, A.; Bour, C.; Suffert, J. *J. Am. Chem. Soc.* **2005**, *127*, 7171. (b) Mota, A. J.; Dedieu, A. *J. Org. Chem.* **2007**, *72*, 9669.

(26) (a) Cámpora, J.; López, J. A.; Palma, P.; Valerga, P.; Spillner, E.; Carmona, E. *Angew. Chem., Int. Ed.* **1999**, *38*, 147. (b) Catellani, M.; Cugini, F.; Bocelli, G. *J. Organomet. Chem.* **1999**, *584*, 63. (c) Karig, G.; Moon, M.-T.; Thasana, N.; Gallagher, T. *Org. Lett.* **2002**, *4*, 3115. (d) Huang, Q.; Fazio, A.; Dai, G.; Campo, M. A.; Larock, R. C. *J. Am. Chem. Soc.* **2004**, *126*, 7460. (e) Zhao, J.; Campo, M.; Larock, R. C. *Angew. Chem., Int. Ed.* **2005**, *44*, 1873. (f) Kesharwani, T.; Larock, R. C. *Tetrahedron* **2008**, *64*, 6090.

(27) Ma, S.; Gu, Z. *Angew. Chem., Int. Ed.* **2005**, *44*, 7512.

Scheme 5. Overall Mechanism Based on Experimental and Computational Results (L = P<sup>t</sup>Bu<sub>3</sub>)

overall mechanism for formation of **2c** from **1c** (Scheme 5). Only coordination of the base *cis* to the aromatic ring would allow such a transformation. In the products of C–H activation resulting from coordination *trans* to the aryl (**12c**, see Figure 4), the steric bulk introduced by P<sup>t</sup>Bu<sub>3</sub> would impede any interaction between the formed O–H and the aromatic carbon bonded to Pd. In the product from C–H activation with the base coordinated *cis* (**14c**), the steric bulk of the phosphine is not interfering with the proton transfer to the aromatic ring (see Figure 7). Moreover the observation of the 1,4-palladium migration and the proposal of a base-assisted mechanism for such transformation is a strong support for the intramolecular C–H activation by an external base and would be more difficult to explain if an intermolecular deprotonation with a noncoordinated base were to be operative.

## Conclusions

We reported on an efficient catalytic system for the synthesis of benzocyclobutenes by C–H activation of methyl groups. The most general conditions were found with a combination of Pd(OAc)<sub>2</sub> and P<sup>t</sup>Bu<sub>3</sub> as catalyst, K<sub>2</sub>CO<sub>3</sub> as the base, and DMF as solvent. A variety of substituted BCB were obtained using this method with yields in the 44–92% range, including molecules that are hardly accessible by other methods. The reaction was found limited to substrates bearing a quaternary benzylic carbon, but BCB bearing a tertiary benzylic carbon could be obtained indirectly from diesters by decarboxylation. Reaction substrates bearing a small substituent *para* to bromine gave an unexpected regioisomer that likely arose from a 1,4-palladium migration process. The formation of this “abnormal” regioisomer could be suppressed by introducing a larger substituent *para* to bromine. Given the synthetic interest of BCB in pericyclic reactions via their *o*-xylylene form, this work should open new perspectives in the chemistry of BCB and their use for the construction of polycyclic molecules.

DFT calculations on the reaction mechanism highlighted important features associated to this transformation. The bulk of the phosphine is not only necessary to create a monoligated Pd<sup>0</sup> complex as the active species, it also allows for a  $\kappa^1$ -coordination of the base *cis* to the metallated aromatic ring. This geometry prevents the formation of very stable  $\kappa^2$ -adducts of the base that would make the C–H activation step difficult.

In the  $\kappa^1$ -adduct, the proton transfer from the sp<sup>3</sup> carbon is computed to be easier for carbonate compared to bicarbonate and acetate, in agreement with the experimental results. The lower activation barrier is the result of both a higher basicity and a smaller electronic reorganization of the coordinated base upon protonation. Dissociation of the protonated base generates an unsaturated metallacycle from which C–C coupling to form the benzocyclobutene is effective. The activation barrier for C–C coupling is lower than the one for C–H cleavage, thus setting the latter process as the rate-limiting step in agreement with the experimental kinetic isotope effect. The  $\kappa^1$ -coordination of the base *cis* to the aromatic ring gives access to a competitive pathway. The proton on the base can be transferred to the aromatic ring, thus yielding an alkyl intermediate. The transfer is reversible and, finally, the BCB is obtained, but rotation of the phenyl ring in the alkyl intermediate gives access to the other regioisomer. This product results formally from a 1,4-migration of Pd and the mechanism presented therein (Scheme 5) could be more general and could allow to explain other 1,4-migrations of palladium observed experimentally.

## Experimental Section

**General C–H Activation Procedure (Table 2).** A dry resealable Schlenk tube containing a magnetic rod was charged with the aryl bromide (1 mmol), Pd(OAc)<sub>2</sub> (0.1 equiv), P(*t*-Bu)<sub>3</sub>·HBF<sub>4</sub> (0.2 equiv), and dry K<sub>2</sub>CO<sub>3</sub> (1.3 equiv). The Schlenk tube was evacuated and backfilled with argon twice, then capped with a rubber septum. Dry DMF (4.0 mL) was injected under argon, then the septum was replaced by a screwcap and the mixture was stirred at 140 °C (preheated oil bath) until disappearance of the starting material in GCMS analysis (generally 1 to 1.5 h). After cooling, the mixture was diluted with Et<sub>2</sub>O and filtered through Celite. The organic solution was washed with brine, dried over MgSO<sub>4</sub>, and the solvent evaporated under reduced pressure. The residue was purified by flash chromatography to afford the benzocyclobutene.

**Computational Details.** The calculations were performed with the Gaussian03 package<sup>28</sup> at the B3PW91 level.<sup>29</sup> Palladium was represented by the relativistic effective core potential (RECP) from the Stuttgart group and the associated basis set,<sup>30</sup> augmented by a

(28) Pople, J. A. et al. *Gaussian 03*, revision C.02; 2003.

(29) (a) Becke, A. D. *J. Chem. Phys.* **1993**, *98*, 5648. (b) Perdew, J. P.; Wang, W. *Phys. Rev. B* **1992**, *45*, 13244.

f polarization function.<sup>31</sup> Bromine and phosphorus were represented by the relativistic effective core potential (RECP) from the Stuttgart group and the associated basis set,<sup>32</sup> augmented by a d polarization function.<sup>33</sup> A 6-31G(d,p) basis set was used for all the other atoms (C, H, O).<sup>34</sup> The geometry optimizations were performed without any symmetry constraint followed by analytical frequency calculations to confirm that a minimum or a transition state had been reached. The nature of the species connected by a given transition state structure was checked by optimization as minima of slightly altered TS geometries along both directions of the transition state vector. The energies of all the systems studied at the B3PW91 level in gas phase were computed with inclusion of solvent effects (DMF) according to the PCM scheme as implemented in Gaussian. The

geometries obtained in gas phase were used without further reoptimization within the PCM methodology<sup>35</sup> and the united atom topological model with UAKS radii was used. Optimizations in solvent have been shown by Senn and Ziegler to yield qualitative difference in C-X oxidative addition reactions,<sup>22f</sup> but in the present study, attempts to converge geometry optimizations within PCM failed.

**Acknowledgment.** This work was financially supported by Institut de Recherche Servier (fellowships to R.P. and N.A.), ICSN (fellowships to M.C. and J.H.), and CNRS (ATIP grant to O.B.).

**Supporting Information Available:** Full characterization of all new compounds, detailed experimental procedures, copies of NMR spectra for target benzocyclobutenes and X-ray crystal structure data (CIF) for compound **2z**. Complete ref 28 and Cartesian coordinates of all optimized structures. This material is available free of charge via the Internet at <http://pubs.acs.org>.

JA805598S

- 
- (30) Andrae, D.; Haussermann, U.; Dolg, M.; Stoll, H.; Preuss, H. *Theor. Chim. Acta* **1990**, *77*, 123.
- (31) Ehlers, A. W.; Bohme, M.; Dapprich, S.; Gobbi, A.; Hollwarth, A.; Jonas, V.; Kohler, K. F.; Stegmann, R.; Veldkamp, A.; Frenking, G. *Chem. Phys. Lett.* **1993**, *208*, 111.
- (32) Bergner, A.; Dolg, M.; Kuchle, W.; Stoll, H.; Preuss, H. *Mol. Phys.* **1993**, *80*, 1431.
- (33) Hollwarth, A.; Bohme, M.; Dapprich, S.; Ehlers, A. W.; Gobbi, A.; Jonas, V.; Kohler, K. F.; Stegmann, R.; Veldkamp, A.; Frenking, G. *Chem. Phys. Lett.* **1993**, *208*, 237.
- (34) Hariharan, P. C.; Pople, J. A. *Theor. Chim. Acta* **1973**, *28*, 213.

- 
- (35) Tomasi, J.; Mennucci, B.; Cammi, R. *Chem. Rev.* **2005**, *105*, 2999.